Phase separation of a binary fluid in the presence of immobile particles: A lattice Boltzmann approach

Domenico Suppa, Olga Kuksenok, and Anna C. Balazs
Department of Chemical and Petroleum Engineering, University of Pittsburgh, Pittsburgh, Pennsylvania 15261

J. M. Yeomans
Theoretical Physics, University of Oxford, Keble Road, Oxford, OX1 3NP, United Kingdom

(Received 14 August 2001; accepted 23 January 2002)

Using a lattice Boltzmann model, the phase separation of a binary fluid in the presence of immobile, penetrable particles is studied in two dimensions. The particles are preferentially wetted by one of the fluid components. At early times, the hydrodynamic flow promotes the growth of the fluid domains. At later times, the domains are pinned to a finite size if there is a sufficiently strong interaction between the particles and the compatible fluid. The final size of the domains depends on the specific strength of the particle–fluid interaction and on the particle concentration. These results indicate that the domain size can be tailored by varying the chemical nature and the number of the particles. © *2002 American Institute of Physics.* [DOI: 10.1063/1.1460863]

I. INTRODUCTION

Polymeric materials are commonly composed of incompatible fluids and thus the phase-separation dynamics of the system plays a crucial role in determining their properties and practical utility.[1,2] Without hydrodynamics, the general characteristics of the phase ordering process for binary mixtures are well understood.[3–5] The growth of the domain size $R(t)$ with time t can be characterized by a single scaling relationship, the well-known Lifshitz–Slyozov law $R(t) \sim t^{1/3}$, which is indicative of purely diffusive transport.[6] When hydrodynamic effects are important, the situation becomes more complex. Now $R(t) \sim t^{\alpha}$, where the value of α depends on the nature of the hydrodynamic regime[7,8] and on the dimensionality (i.e., 2D versus 3D) of the system. However, both theoretical scaling arguments[9,10] and computer simulations[11,12] indicate that hydrodynamic flow, driven by interfacial tension, leads to a value of α that is $>1/3$.[13]

The introduction of particles or ''fillers'' into a fluid mixture complicates the phase-separation dynamics even further. Even the presence of *immobile* particles in thin films of phase-separating fluids has experimentally been shown to yield novel kinetic and structural properties.[14,15] It is important to understand the behavior of these complex mixtures since the particles can provide a useful means of controlling the morphology of the system and thus, tailoring the properties of the composite. The hydrodynamic behavior of a binary, phase-separating mixture containing stationary, penetrable particles has recently been investigated in two dimensions.[13] In the latter paper, the authors explicitly solve a modified Navier–Stokes equation for the binary fluid/soft particle system. Their findings indicate that in the late stage of the coarsening process, particles that are preferentially favored by one of the fluids can cause the domains to be pinned at a finite size.

In this paper, we characterize a binary fluid/particle mixture through a similar free energy functional as in Ref. 13, but now house this expression in a lattice Boltzmann approach. Using this approach, we recover the previous predictions for the effect of stationary particles on the characteristic domain size and thus demonstrate that the lattice Boltzmann model provides an effective method for investigating the hydrodynamic behavior of a binary fluid in the presence of immobile particles. We then use the model to vary the strength of the interaction between the particles and favored fluid component, and show that the domain size can be tailored by altering the chemical nature of the particles.

II. THE MODEL

The system consists of a 50:50 A/B binary mixture and immobile impurity sites, or particles. The fluid is characterized by the order parameter $\phi(\mathbf{r},t)=\rho_A(\mathbf{r},t)-\rho_B(\mathbf{r},t)$, which is the difference in the local number density of A and B. The particles in the system are ''soft'' or penetrable since we neglect excluded volume interactions between the particles and the fluids. This can be a valid approximation for small (i.e., nanoscale) particles. The thermodynamic behavior of the system is described by the following free energy functional:

$$F[\phi]=F_{\mathrm{G.L.}}[\phi]+\sum_{i=1}^{N} U_i[\phi], \tag{1}$$

where $F_{\mathrm{G.L.}}$ is the usual Ginzburg–Landau free energy,

$$F_{\mathrm{G.L.}}[\phi]=\int d\mathbf{r}\left(-\frac{\tau}{2}\phi^2+\frac{u}{4}\phi^4+\frac{k}{2}|\nabla\phi|^2\right) \tag{2}$$

and $u>0$ and $k>0$ are phenomenological parameters. The term $k/2|\nabla\phi|^2$ represents the free energy cost of forming fluid–fluid interfaces. For $\tau<0$, $F_{\mathrm{G.L.}}$ describes a single homogeneous phase, while for $\tau>0$, it yields two-phase coexistence. Neglecting fluctuations, one finds $\phi_{\mathrm{eq}}=(\tau/u)^{1/2}$ with ϕ_{eq} corresponding to the equilibrium order parameter for the

A-rich phase, and $-\phi_{\mathrm{eq}}$ corresponding to the order parameter for the *B*-rich phase. In the studies described here, we choose $\phi_{\mathrm{eq}}=1$. The term $U_i[\phi]$ is a potential that describes the coupling interaction between the ith impurity center located at $\mathbf{s}_i$ and the surrounding fluid,

$$U_i[\phi]=\int d\mathbf{r}V_0 e^{-(|\mathbf{r}-\mathbf{s}_i|/r_0)}(\phi(\mathbf{r})-\phi(\mathbf{s}_i))^2. \tag{3}$$

The summation in Eq. (1) is over the total number of particles, N. The constant $V_0>0$ characterizes the strength of the coupling interaction and r_0 represents its range, which is chosen to be much less than the domain size and comparable to the thickness of the interface. The parameter r_0 effectively sets the size of the penetrable particle. The particles favor one component of the mixture and thus, act as osmotic force centers. By setting $\phi(\mathbf{s}_i)=\phi_{\mathrm{eq}}=1$ for all $i\in(1,...,N)$, we model the fact that the particles favor the *A*-phase. Small, long-wavelength deviations of the order parameter from its equilibrium value may be described by the equations of linearized hydrodynamics.[16–18] In the overdamped limit (where the fluid velocity is slow), the equations reduce to the following:[17,18]

$$\frac{\partial}{\partial t}\phi(\mathbf{r},t)+\nabla\cdot(\mathbf{v}(\mathbf{r},t)\phi(\mathbf{r},t))=M\nabla^2\frac{\delta F}{\delta\phi(\mathbf{r},t)}, \tag{4}$$

$$0=-\nabla p+\eta\nabla^2\mathbf{v}(\mathbf{r},t)+\frac{\delta F}{\delta\phi}\nabla\phi(\mathbf{r},t), \tag{5}$$

where M is a mobility coefficient and η is the shear viscosity. The parameter p is a Lagrange multiplier that guarantees the incompressibility condition, $\nabla\cdot\mathbf{v}=0$. These equations can be rewritten in nondimensional units by choosing the scale of length to be $\xi=(k/\tau)^{1/2}$, which is proportional to the thickness of the interface, the scale of time as $t_D=\xi^2/\tau M$, which represents the diffusion time across the interface, and $\phi_{\mathrm{eq.}}$ as the order parameter scale.[13] In the rescaled variables, the two coupled equations can be written as

$$\frac{\partial}{\partial t}\phi(\mathbf{r},t)=-\nabla\cdot(\mathbf{v}(\mathbf{r},t)\phi(\mathbf{r},t))+\nabla^2\frac{\delta F}{\delta\phi(\mathbf{r},t)}, \tag{6}$$

$$0=-\nabla P+\nabla^2\mathbf{v}(\mathbf{r},t)+C\frac{\delta F}{\delta\phi}\nabla\phi(\mathbf{r},t), \tag{7}$$

where the parameter $C=(\phi_{\mathrm{eq.}}^2 k)/(\eta M\tau)$ is the capillary number, which measures the significance of the hydrodynamic effects.

III. LATTICE BOLTZMANN ALGORITHM

Equations (6) and (7) are solved numerically through a lattice Boltzmann algorithm.[19–21] There are several advantages of using lattice Boltzmann algorithms over more conventional computational fluid dynamics techniques. These include the simplicity of programming and the capability of incorporating complex microscopic interactions in a straightforward way. In this work, we exploit these features to develop the first lattice Boltzmann algorithm for modeling a binary mixture that contains immobile particles.

The lattice Boltzmann algorithm describes the evolution of single-particle density distribution functions on the sites of a regular lattice. Here, we work on a two-dimensional, square lattice. To model a binary fluid consisting of *A* and *B* particles of respective densities ρ_A and ρ_B, two sets of distribution functions, f_i and g_i, are defined on each lattice site $\mathbf{r}$. Each f_i, g_i, is associated with a lattice vector $\mathbf{e}_i=(\pm1,0)$, $(0,\pm1)$, $(\pm1,\pm1)$, $(0,0)$. The distribution functions f_i are related to the transport of mass and momentum in the system; the g_i are related to the changes in composition within the mixture. The distribution functions satisfy the following equations:

$$\rho=\sum_i f_i, \quad \rho u_\alpha=\sum_i f_i e_{i\alpha}, \quad \phi=\sum_i g_i, \tag{8}$$

where the total number density is $\rho=\rho_A+\rho_B$, the number density difference is $\phi=\rho_A-\rho_B$, and $\mathbf{u}$ is the bulk fluid velocity. The α subscripts in the above equation represent Cartesian coordinates. In these calculations, the mass is set equal to one.

The distribution functions at each lattice site are updated at each time step Δt. The evolution equations for the distribution functions obey an extension of a Bhatnagar–Gross–Krook predictor-corrector scheme (see Ref. 22):

$$f_i(\mathbf{x}+\mathbf{e}_i\Delta t,t+\Delta t)-f_i(\mathbf{x},t)=\frac{\Delta t}{2}[\mathcal{C}_{fi}(\mathbf{x},t,\{f_i\})+\mathcal{C}_{fi}(\mathbf{x}+\mathbf{e}_i\Delta t,t+\Delta t,\{f_i^*\})], \tag{9}$$

$$g_i(\mathbf{x}+\mathbf{e}_i\Delta t,t+\Delta t)-g_i(\mathbf{x},t)=\frac{\Delta t}{2}[\mathcal{C}_{gi}(\mathbf{x},t,\{f_i\})+\mathcal{C}_{gi}(\mathbf{x}+\mathbf{e}_i\Delta t,t+\Delta t,\{g_i^*\})], \tag{10}$$

where f_i^* and g_i^* are first order approximations to $f_i(\mathbf{x}+\mathbf{e}_i\Delta t,t+\Delta t)$ and $g_i(\mathbf{x}+\mathbf{e}_i\Delta t,t+\Delta t)$, respectively. The operators $\mathcal{C}_{fi}(\mathbf{x},t,\{f_i\})$ and $\mathcal{C}_{gi}(\mathbf{x},t,\{g_i\})$ are defined by the following equations:

$$\mathcal{C}_{fi}(\mathbf{x},t,\{f_i\})=-\frac{1}{\tau_f}(f_i(\mathbf{x},t)-f_i^{\mathrm{eq}}(\mathbf{x},t,\{f_i\}))+h_i(\mathbf{x},t,\{f_i\}), \tag{11}$$

$$\mathcal{C}_{gi}(\mathbf{x},t,\{g_i\})=-\frac{1}{\tau_g}(g_i(\mathbf{x},t)-g_i^{\mathrm{eq}}(\mathbf{x},t,\{g_i\})). \tag{12}$$

The f_i^{eq} and g_i^{eq} are equilibrium distribution functions that determine the physics inherent in the simulation, and h_i allows us to model the presence of extra forces acting on the system. The equilibrium distribution functions and the h_i term are defined through the following expansions:[20,21]

$$\begin{aligned} f_i^{\mathrm{eq}}&=A+Bu_\alpha e_{i\alpha}+Cu^2+D_s u_\alpha u_\beta e_{i\alpha}e_{i\beta}+G_{\alpha\beta}e_{i\alpha}e_{i\beta},\\ g_i^{\mathrm{eq}}&=L+Ku_\alpha e_{i\alpha}+Ju^2+Qu_\alpha u_\beta e_{i\alpha}e_{i\beta},\\ h_i&=TH_\alpha e_{i\alpha}. \end{aligned} \tag{13}$$

The coefficients in these equations are determined by the conservation of density, momentum and density difference,

$$\sum_i f_i^{eq} = \rho, \quad \sum_i f_i^{eq} e_{i\alpha} = \rho u_\alpha, \quad \sum_i g_i^{eq} = \phi, \tag{14}$$

together with

$$\sum_i f_i^{eq} e_{i\alpha} e_{i\beta} = P_{\alpha\beta} + \rho u_\alpha u_\beta, \tag{15}$$

$$\sum_i g_i^{eq} e_{i\alpha} e_{i\beta} = \Gamma_{\mu_\phi} \delta_{\alpha\beta} + \phi u_\alpha u_\beta, \tag{16}$$

and

$$\sum_i h_i = 0, \ \sum_i h_i e_{i\alpha} = H_\alpha, \ \sum_i h_i e_{i\alpha} e_{i\beta} = 0. \tag{17}$$

The term $H_\alpha(\mathbf{r}) = -\phi \nabla_\alpha \Sigma_{i=1}^N \delta U_i[\phi]/\delta\phi$ represents the α-component of the force at point $\mathbf{r}$ due to the particles, and Γ is proportional to the mobility ($M = \Gamma \tau_g$). Note the appearance of the tensor $P_{\alpha\beta} = p_0 \delta_{\alpha\beta} + k[\partial_\alpha \phi \partial_\beta \phi - (\phi \nabla^2 \phi + \frac{1}{2}(\nabla\phi)^2)\delta_{\alpha\beta}]$ in Eq. (15), where p_0 is a bulk pressure consistent with its thermodynamic definition,[21] and of the chemical potential $\mu_\phi = \delta F/\delta\phi$ in Eq. (16). These parameters incorporate the equilibrium properties of the mixture into the dynamic equations for the structural evolution of the system.

With the above constraints, expansion of Eqs. (9)–(10), up to second order in Δt, leads in the continuum limit to both Eq. (4) and the Navier–Stokes equation, usually written in the form,[21–23]

$$\rho \partial_t(\mathbf{v}) + \rho(\mathbf{v}\nabla)\mathbf{v} = -\nabla \mathbf{P} + \eta \Delta \mathbf{v} + \mathbf{H}, \tag{18}$$

where viscosity is defined as $\eta = \rho \tau_f/3$ and $\mathbf{P}$ is a tensor with components $P_{\alpha\beta}$. We choose parameters in our simulations to ensure that the equations are in the overdumped limit (which is appropriate for most experimental system[17]), so that we can neglect the l.h.s. of Eq. (18). The r.h.s. of this equation can be rewritten in the same form as Eq. (5).[24] Thus, using the algorithm described here, we are looking for a solution to the system of Eqs. (4) and (5).

IV. RESULTS AND DISCUSSIONS

The lattice Boltzmann simulations described above were carried out in two dimensions, on a lattice 256×256 sites in size. The particles were introduced into the system at randomly chosen sites and remained fixed during the phase separation of the binary mixture. In the plots shown below, each data point represents an average over three independent runs. (To test for finite size effects, simulations were also run on 64×64 and 128×128 site lattices; calculations on all three lattices gave essentially identical values for the domain sizes.) The numerical values of the parameters that appear in the free energy [Eqs. (2) and (3)] are $\tau = u = 0.01$, $k = 0.02$, $V_0 = 0.0025$, and $r_0 = 1$. Together with a number density $\rho = 1$ and a mobility $M = 1$, these values guarantee that the we are in the overdamped limit of the hydrodynamic behavior, as described by Eq. (7), for all values of the capillary number considered in our study.[25] Moreover, the forces due to the particles represent a small, short range perturbation in the system.

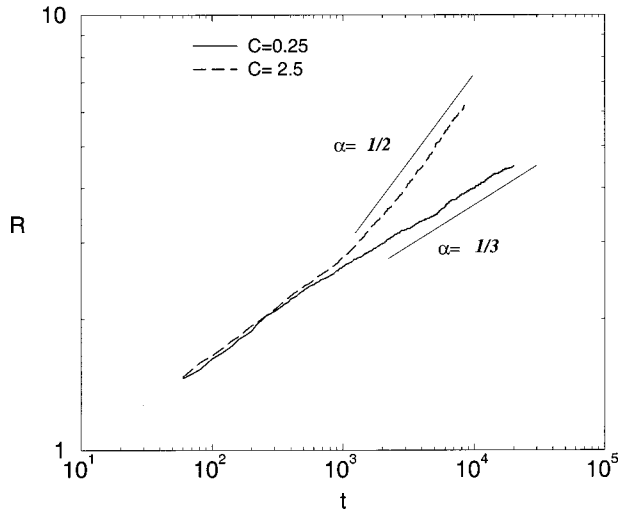

FIG. 1. Characteristic domain size R vs time t for the pure binary mixture. Small values of the capillary number do not modify the usual Lifshitz–Slyozov Law; for capillary number $C = 2.5$, the growth exponent is modified by hydrodynamic effects.

In the absence of particles and hydrodynamics, our results are consistent with the Lifshitz–Slyozov growth law for the domain size, i.e., $R(t) \sim t^{1/3}$. This growth law is also observed for small values of the capillary number C, up to a value of approximately 0.25. The hydrodynamic effects become apparent for an intermediate range of C's, where the scaling exponent grows continuously from 1/3 to 1/2. The value of 1/2 for the scaling exponent is reached at $C = 1$ and this value remains stable, at least over the range of times considered, for even higher values of C (the largest value considered here was $C = 50$). The two limiting situations are shown in Fig. 1 and agree with those obtained in Ref. 13. In Fig. 2, 3, and 4, the morphologies of the system are shown at different times and strength of the coupling (values of V_0) between the soft particles and fluid. As was also observed in Ref. 13, the introduction of the soft particles strongly modifies the coarsening of the domains and gives rise to a saturation of their size at late times. We also note that increasing the coupling constant V_0 decreases the pinned value of the domain size, as can be seen by comparing Figs. 3 and 4. We will return to this point at the end of this section.

In order to characterize the behavior of the system, we adopt the theoretical model introduced in Ref. 13. At late times, we can consider the system as being partitioned into a large number of domains of characteristic length R. Because the particles are randomly distributed on the lattice and the forces due to the particles are short ranged, it can be argued that the values of the particle density in the different domains approximately obey a Gaussian distribution, centered at $n_0 = N/L^2$, where L is the length of the simulation box, and having a variance $\sigma_e^2 = 2n_0/R^2$. In this case, the mean value of the particle density in the unfavorable B-phase, n_-, can be expressed by the following scaling relation:[13]

$$n_-(R) = n_0 F(R/R_0), \tag{19}$$

where $R_0 = (2/n_0)^{1/2}$ and the scaling function is $F = \mathrm{erf}(x) - (1 - \exp(-x^2))/(\pi^{1/2} x)$ (where erf is the error function).

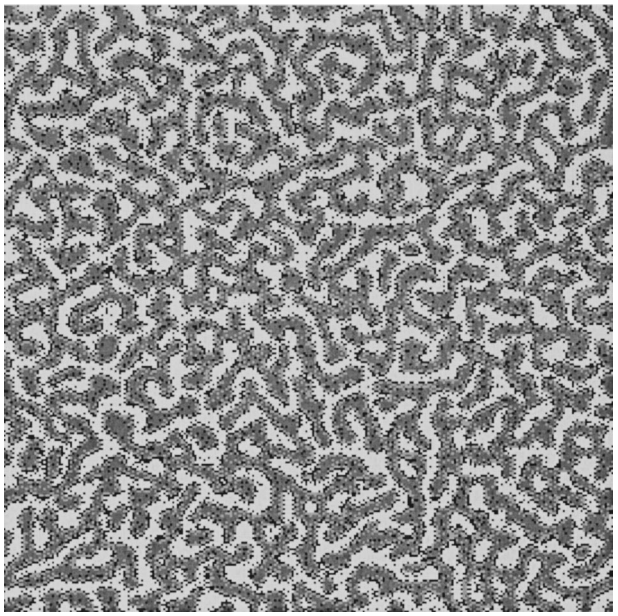

FIG. 2. Morphology of the binary fluid containing $N=3200$ immobile particles in the presence of hydrodynamics ($C=0.25$) at early times ($t=1000$). Dark gray corresponds to the *A*-phase, light gray corresponds to the *B*-phase, and the black points represent the particles.

Hence, the particle number density in the *B*-phase should be determined by the dimensionless number R/R_0 and the total number density of particles in the system. To verify the above scaling form, in Fig. 5 we collapse the data obtained from the simulations by plotting $Y=n_-/n_0$ against $X=R/R_0$. It is seen that, for different total particle densities, all the data fit fairly well onto one master curve without any adjustable parameters.

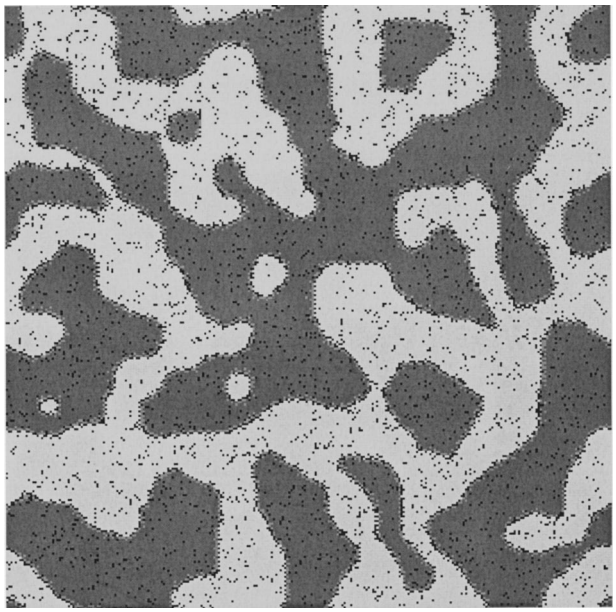

FIG. 3. Morphology of the binary fluid containing $N=3200$ immobile particles in the presence of hydrodynamics ($C=0.25$) at late times ($t=10\,000$); the coupling constant V_0 is set equal to 0.0025. Dark gray corresponds to the *A*-phase, light gray corresponds to the *B*-phase, and the black points represent the particles.

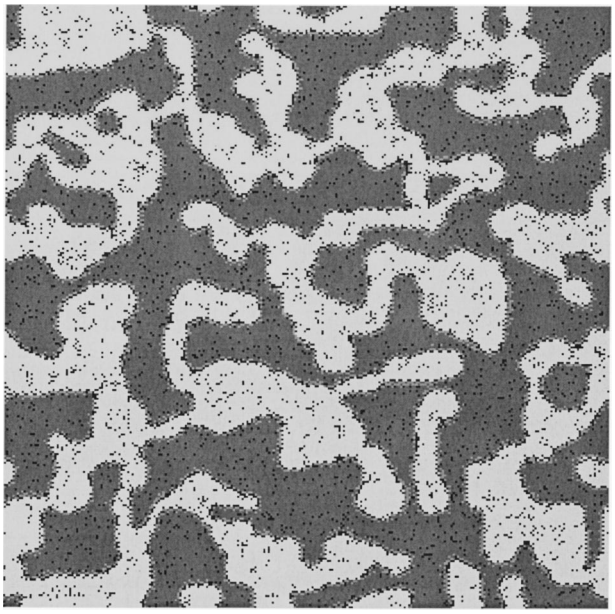

FIG. 4. Morphology of the binary fluid containing $N=3200$ immobile particles and in the presence of hydrodynamics ($C=0.25$) at late times ($t=10\,000$): the coupling constant V_0 is set equal to 0.005. Dark gray corresponds to the *A*-phase, light gray corresponds to the *B*-phase, and the black points represent the particles.

At the late stage of the evolution, the value of the excess free energy density of the system in two dimensions can be qualitatively estimated as

$$\frac{\Delta F(R)}{L^2} \propto \frac{\sigma}{R} + V_{\mathrm{cpl}} n_-(R), \tag{20}$$

i.e., as the sum of an interfacial free energy σ/R (where σ is related to the mean value of the surface tension) and a mean energy penalty $V_{\mathrm{cpl}} \propto (2\phi_{\mathrm{eq}})^2 V_0$ for a particle immersed in the *B*-phase, times the mean local density of those particles.

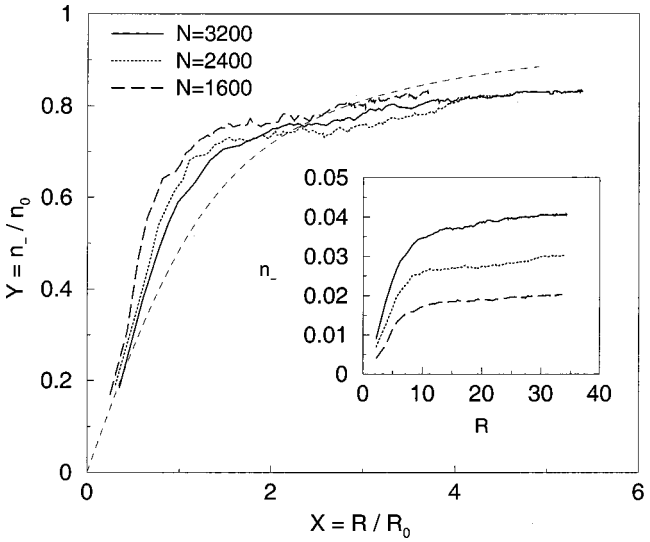

FIG. 5. Immobile particle density in the unfavored phase n_- vs time t for three different mean densities $n=3200/L^2$, $2400/L^2$, $1600/L^2$, where $L=256$. The main picture confirms the scaled form given in Eq. (19); the inset shows the relationship between the original variables. The dashed line is a plot of the function $F=\mathrm{erf}(x)-(1-\exp(-x^2))/(\pi^{1/2}x)$.

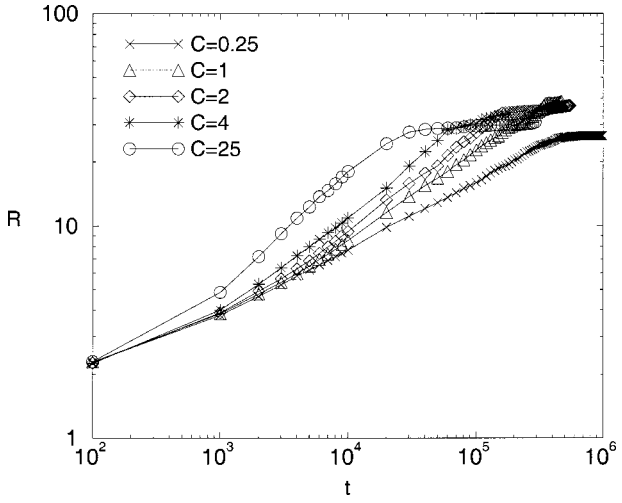

FIG. 6. Evolution in time of the characteristic domain size with $N=3200$ immobile particles, $V_0=0.0025$, $k=0.02$, and different values of the capillary number C.

Minimizing expression (20) with respect to R, it is possible to show that in 2D, the excess free energy has a minimum only if the parameters of the system satisfy the following condition:[13]

$$0<\left(\frac{\pi}{2n_0}\right)^{1/2}\left(\frac{\sigma}{V_{\mathrm{cpl}}}\right)<1. \tag{21}$$

This condition allows us to estimate the maximum ratio between surface tension and coupling constant that gives a saturation of the domain lengths. If this condition is not satisfied, for example if the coupling is too small, the system continues to coarsen like a simple binary fluid without particles.

When the condition in Eq. (20) is satisfied, one has the possibility of tailoring not only the final domain size, but also the rate at which this size is reached. In particular, Fig. 6 shows the effect of hydrodynamics on the domain saturation dynamics for the fixed value of the coupling constant

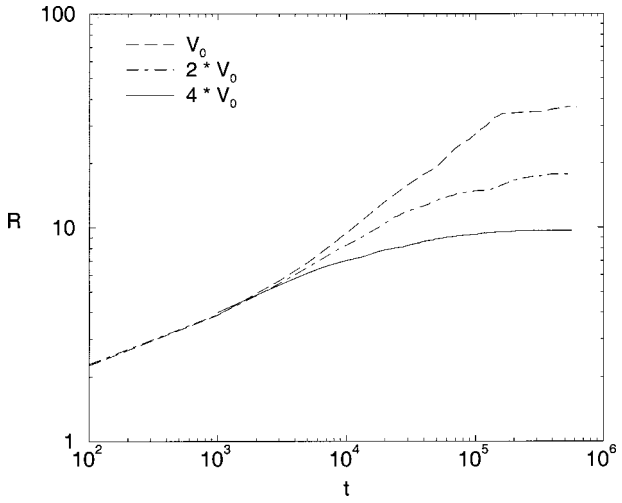

FIG. 7. Evolution in time of the characteristic domain size for three different values of the coupling constant: $V_0=0.0025$, 0.0050, and 0.01. The other relevant parameters are fixed at $N=3200$, $k=0.02$, and $C=2$.

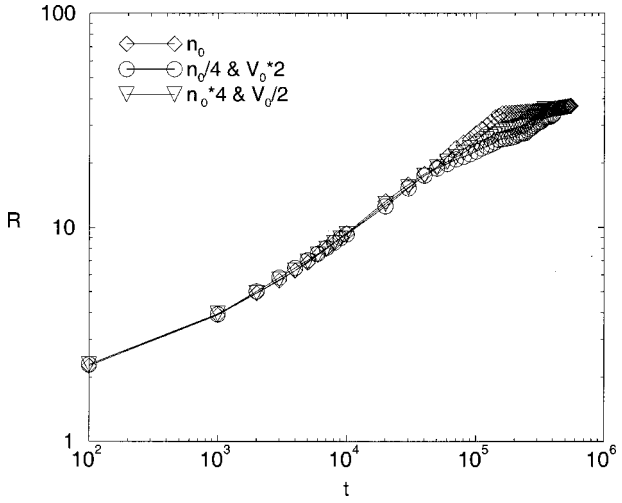

FIG. 8. Evolution in time of the characteristic domain size for different values of the coupling constant and particle concentration with the product $n_0^{1/2}\cdot V_0$ being held constant. Curve 1 corresponds to the reference values $V_0=0.0025$, $n_0=0.05$, $k=0.02$, and $C=2$. The values of the coupling constant and particle concentration are $n_0/4$ and $2V_0$ for curve 2, and $4n_0$ and $V_0/2$ for curve 3.

$V_0=0.0025$. It can be seen that increasing the capillary number C results in a more rapid coarsening of the system to the final domain size; the actual size of the pinned domains remains the same for the various values of C. The final domain size can, however, be altered by varying the coupling constant and the concentration of particles.

In Fig. 7, we plot R as a function of time for three different values of the coupling constant V_0 for a fixed value of C and n_0. Using $V_0=0.0025$ as our reference value, we increase V_0 by a factor of 2 and a factor of 4. For $V_0=0.0050$, the final domain size is half the size (20 lattice units) of the value for $V_0=0.0025$ (40 units), and for the case of $V_0=0.01$, the final domain size is a quarter (10 units) of the reference value.

The final domain size can also be tailored by changing the particle concentration; by halving the value of $(n_0)^{1/2}$, we obtain a twofold increase in the value of final domain size. On the other hand, Fig. 8 shows that if we change both n_0 and V_0 in such a way that the product $(n_0)^{1/2}V_0$ remains constant, we obtain the same value of the saturated domain size.

V. CONCLUSIONS

In this paper, we developed a lattice Boltzmann algorithm to investigate the phase separation process of a binary fluid in the presence of immobile penetrable particles, which are preferentially wetted by one of the fluid components. The coarsening of the domains was studied in the overdamped hydrodynamic regime. In agreement with previous numerical and theoretical studies,[13] we find that the particles can inhibit the growth of the fluid domains for sufficiently high values of the coupling constant V_0. The fact that two independent computational approaches show this behavior provides a convincing argument that stationary particles can have a significant effect on the phase-separation dynamics and morphology of binary fluids. We also note that the pinning of the

domains is in agreement with experimental studies on phase-separation in thin films containing immobile particles that are preferentially wetted by one of the binary fluids.[14,15]

Using the lattice Boltzmann algorithm, we showed that the actual size of the domains can be tailored by varying the strength of the coupling interaction between the particles and the compatible fluid. In physical terms, this effect could be achieved by altering the coating on filler particles or by using chemically different species (e.g., gold versus tin or silver particles) to attain the desired domain size. In addition, we showed that altering the particle concentration provides an alternative means of regulating the final domain size.

The method introduced here provides a computationally efficient means of investigating the effect of stationary filler particles on the structural evolution of multicomponent fluids. It has recently been suggested[26] that interesting phenomena may arise if both *A*-compatible and *B*-compatible particles were added to a binary, phase-separating A/B mixture. The lattice Boltzmann model described here could be used to provide insight into the phase-ordering in this and other complex fluid/particle systems.

ACKNOWLEDGMENTS

A.C.B., O.K., and D.S. are grateful to Professor D. Sherrington for their hospitality in the Theoretical Physics Department of the University of Oxford. The authors also wish to thank A. Wagner, A. Briant, and Professor D. Jasnow for useful discussions. A.C.B. acknowledges financial support from the NSF.

[1] H. Van Oene, in *Polymer Blends*, edited by D. R. Paul and S. Newman (Academic, Orlando, 1978), Vol. 1, Chap. 7.
[2] K. R. Elder, T. M. Rogers, and R. C. Desai, Phys. Rev. B **38**, 4725 (1988).
[3] K. Binder, in *Phase Transformations of Materials, Materials Science, and Technology*, edited by R. W. Cahn, P. Haasen, and E. J. Kramer (VCH, Weinheim, 1991), pp. 5, 405.
[4] A. J. Bray, Adv. Phys. **43**, 357 (1994).
[5] J. D. Gunton, M. San Miguel, and P. Sahni, in *Phase Transition and Critical Phenomena*, edited by C. Domb and J. L. Lebowitz (Academic, London, 1983), Vol. 8, and references therein.
[6] I. M. Lifshitz and V. V. Slyozov, J. Phys. Chem. Solids **19**, 35 (1961).
[7] A. De Masi, E. Orlandi, E. Presutti, and L. Triolo, Nonlinearity **7**, 633 (1994).
[8] Y. Oono and S. Puri, Mod. Phys. Lett. B **2**, 861 (1988).
[9] T. Ohta, D. Jasnow, and K. Kawasaki, Phys. Rev. Lett. **49**, 1223 (1982).
[10] M. San Miguel, M. Grant, and J. D. Gunton, Phys. Rev. A **31**, 1001 (1985); H. Furukawa, *ibid.* **31**, 1103 (1985); T. Keyes and I. Oppenheim, *ibid.* **8**, 937 (1973); Y. Pomeau and P. Rèsibois, Phys. Lett. **19C**, 64 (1975); K. Binder, Phys. Rev. B **15**, 4425 (1977).
[11] A. J. Wagner and J. M. Yeomans, Phys. Rev. Lett. **80**, 1429 (1998); V. M. Kendon, J. C. Desplat, P. Bladon, and M. E. Cates, *ibid.* **82**, 14 (1999).
[12] J. E. Farrel and O. T. Valls, Phys. Rev. B **40**, 7027 (1989); **42**, 2353 (1990); G. Leptoukh, B. Strickland, and C. Roland, Phys. Rev. Lett. **74**, 3636 (1995); W. R. Osborn *et al.*, *ibid.* **75**, 4031 (1995); S. Bastea and J. L. Lebowitz, Phys. Rev. E **52**, 3821 (1995); T. Lookman *et al.*, *ibid.* **53**, 5513 (1996).
[13] F. Qiu, G. Peng, V. Ginzburg, H. Chen, D. Jasnow, and A. C. Balazs, J. Chem. Phys. **115**, 3779 (2001).
[14] H. Tanaka, A. Lovinger, and J. Davis, Phys. Rev. Lett. **72**, 2581 (1994).
[15] A. Karim, J. F. Douglas, G. Nisato, D. W. Liu, and E. Amis, Macromolecules **32**, 5917 (1999).
[16] L. Landau and E. Lifshitz, *Fluid Mechanics* (Pergamon, New York, 1959).
[17] A. J. Bray, Adv. Phys. **43**, 357 (1994).
[18] D. Jasnow and J. Vinals, Phys. Fluids **8**, 660 (1996).
[19] S. Chen and G. D. Doolen, Annu. Rev. Fluid Mech. **30**, 329 (1998).
[20] E. Orlandini, M. R. Swift, and J. M. Yeomans, Europhys. Lett. **32**, 463 (1995).
[21] M. R. Swift, E. Orlandini, W. R. Osborn, and J. M. Yeomans, Phys. Rev. E **54**, 5041 (1996).
[22] C. Denniston, E. Orlandini, and J. M. Yeomans, Europhys. Lett. **52**, 481 (2000); Phys. Rev. E **64**, 021701 (2001).
[23] O. Kuksenok, J. M. Yeomans, and A. C. Balazs, Phys. Rev. E **65**, 031502 (2002).
[24] The r.h.s. of Eq. (18) can be rewritten as $-\nabla \mathbf{P} + \eta \Delta \mathbf{v} + \mathbf{H} = -\nabla p_0 + \eta \Delta \mathbf{v} - \phi \nabla(\delta F/\delta \phi) = -\nabla p + \eta \Delta \mathbf{v} + (\delta F/\delta \phi)\nabla \phi$, where we made the subsitution $p = p_0 + \phi(\delta F/\delta \phi)$.
[25] These values of the parameters differ from those used in Ref. 11. In particular, we use a smaller value of the mean density ρ and a higher value of the surface tension parameter k. If we use the parameters in (Ref. 11), we recover the same value of the scaling exponent as in that paper.
[26] H. Tanaka, J. Phys.: Condens. Matter **13**, 4637 (2001).